

Supporting Information

**Reverse saturable absorbing cationic iridium(III) complexes bearing 2-(2-quinolinyl)quinoxaline ligand: Effects of different cyclometalating ligands on the linear and nonlinear absorption**

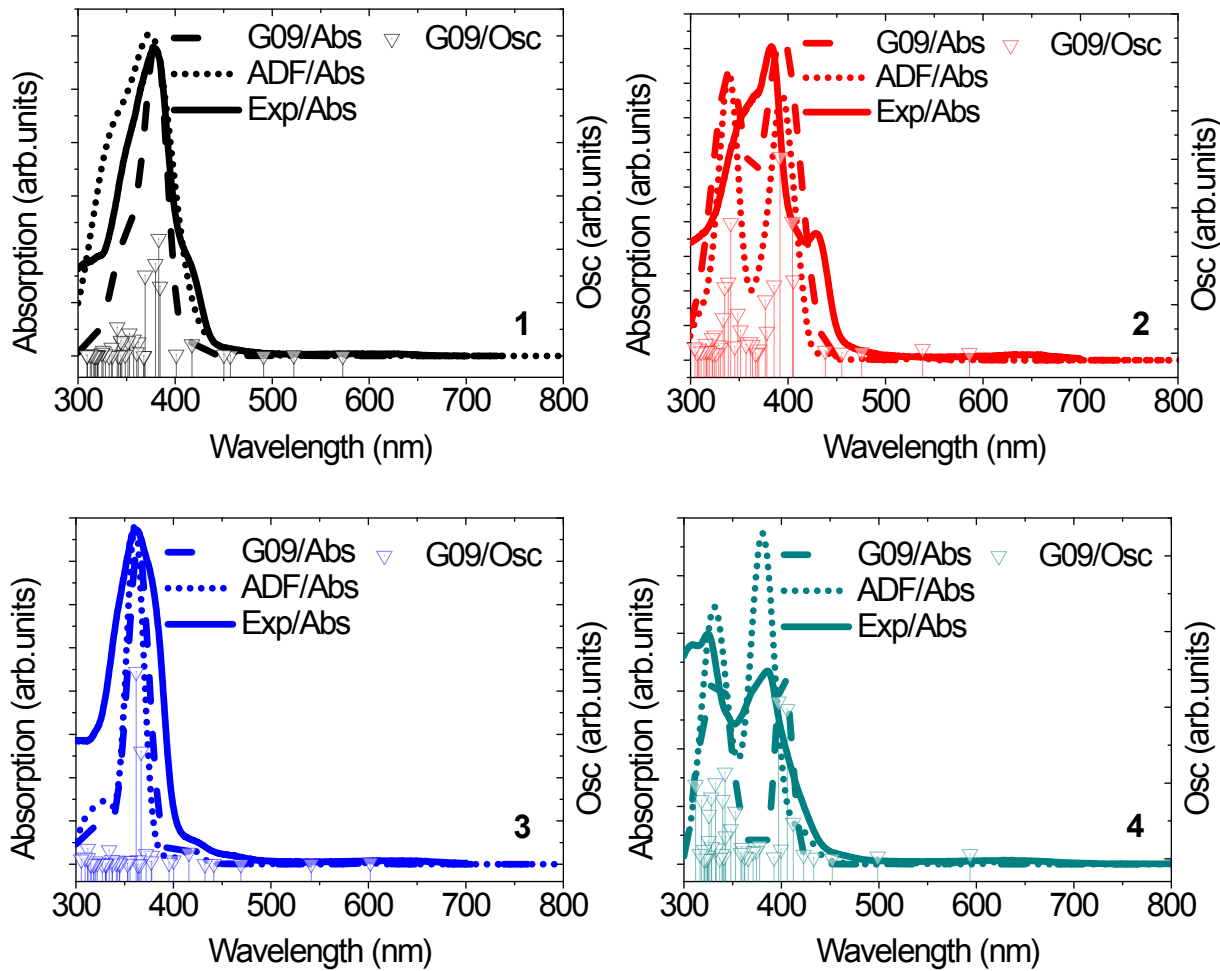
Wenfang Sun,<sup>a,\*</sup> Chengkui Pei,<sup>a</sup> Taotao Lu,<sup>a</sup> Peng Cui,<sup>a,b</sup> Zhongguo Li,<sup>c</sup> Christopher McCleese,<sup>d</sup> Yu Fang,<sup>c</sup> Svetlana Kilina,<sup>a</sup> Yinglin Song,<sup>c</sup> Clemens Burda<sup>d</sup>

<sup>a</sup> Department of Chemistry and Biochemistry, North Dakota State University, Fargo, North Dakota 58108-6050, USA.

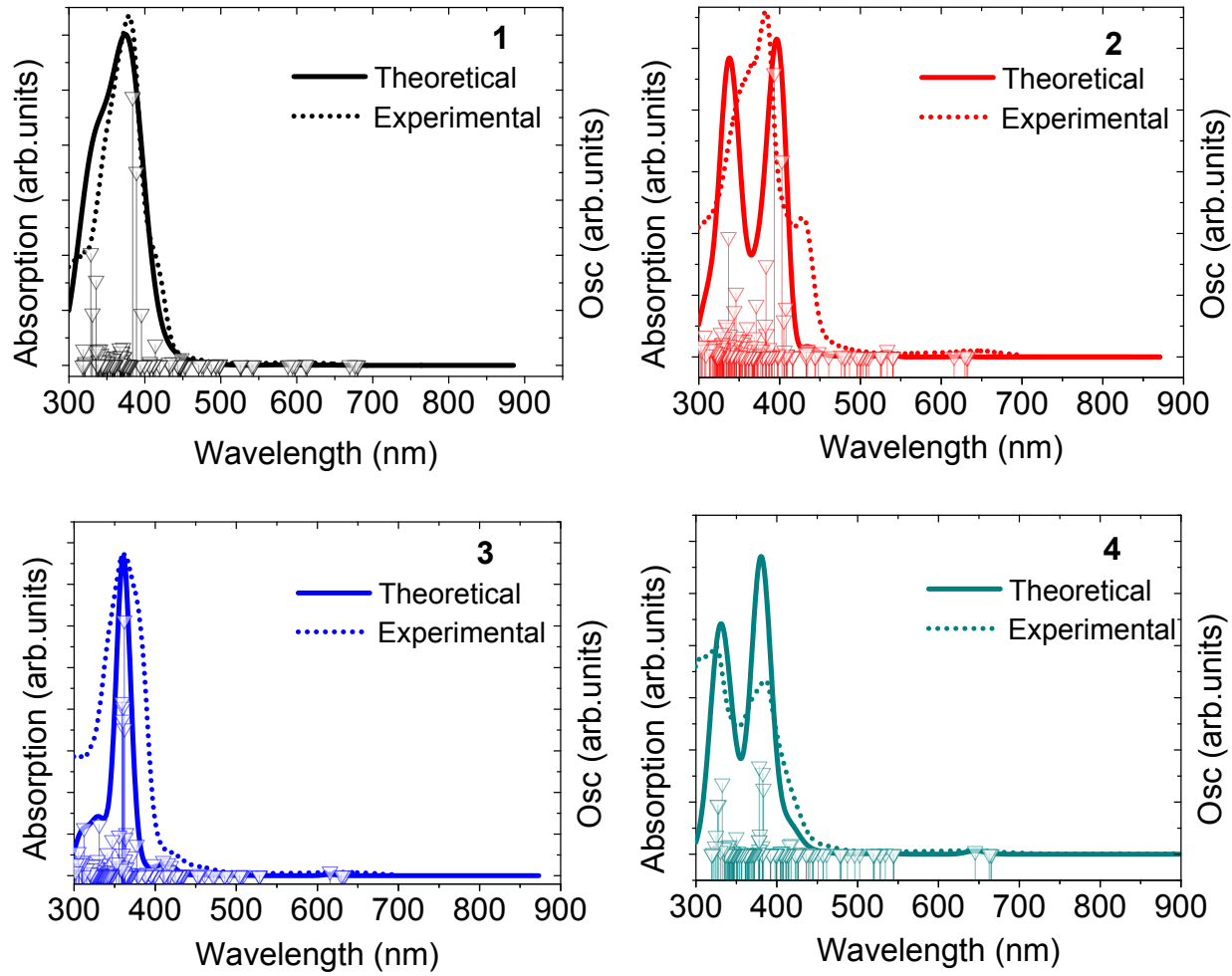
<sup>b</sup> Materials and Nanotechnology Program, North Dakota State University, Fargo, North Dakota 58108-6050, USA

<sup>c</sup> School of Physical Science and Technology, Soochow University, Soochow 215006, P. R. China

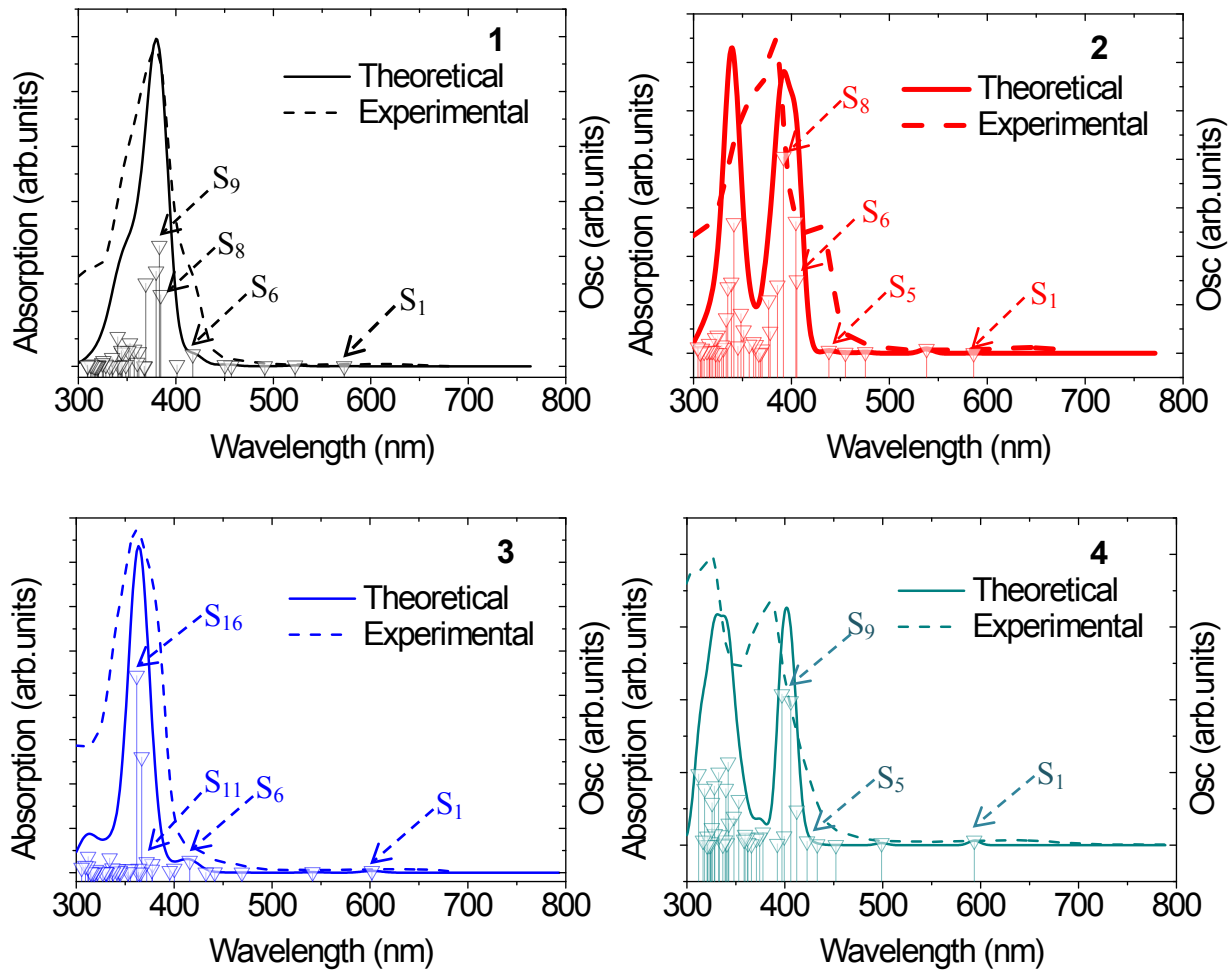
<sup>d</sup> Department of Chemistry, Case Western Reserve University, Cleveland, Ohio 44106, USA



**Figure S1.** Comparison of UV-vis absorption spectra of **1 – 4** in  $\text{CH}_2\text{Cl}_2$  calculated by Gaussian09 (dashed line) and ADF (dotted line) software packages, respectively. All calculations do not include spin-orbit coupling.

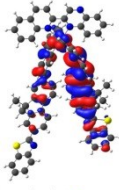
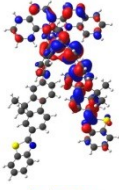
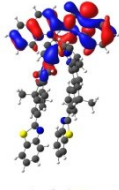
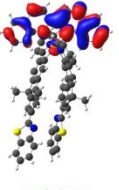
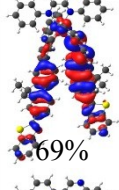
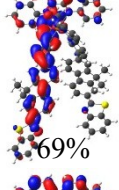
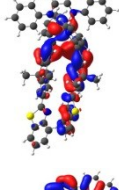
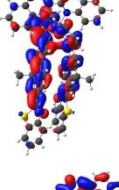
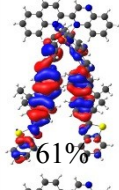
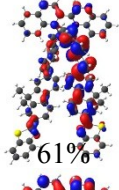
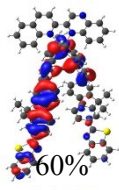
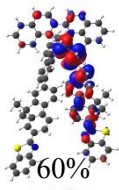
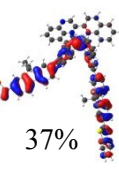
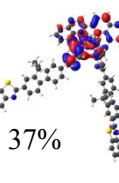
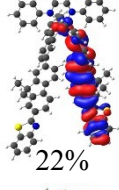
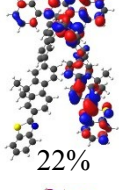


**Figure S2.** Comparison of the experimental and theoretical UV-vis absorption spectra of **1** – **4** in  $\text{CH}_2\text{Cl}_2$  when spin-orbit coupling effect is taken into account.



**Figure S3.** Comparison of the experimental and theoretical UV-vis absorption spectra of **1** – **4** in  $\text{CH}_2\text{Cl}_2$  calculated by Gaussian09 software without spin-orbit coupling.

**Table S1.** Natural transition orbitals (NTOs) representing the high-energy major absorption bands.

Transition states	Hole	Electron	Hole	Electron	
<b>1</b> S <sub>10</sub> 380 nm <i>f</i> = 0.86			<b>2</b> S <sub>19</sub> 348 nm <i>f</i> = 0.17		
S <sub>14</sub> 362 nm <i>f</i> = 0.13	 69%	 69%	S <sub>21</sub> 341 nm <i>f</i> = 0.54		
S <sub>16</sub> 357 nm <i>f</i> = 0.15	 61%	 61%	<b>3</b> S <sub>26</sub> 334 nm <i>f</i> = 0.16		
S <sub>21</sub> 344 nm <i>f</i> = 0.14	 60%	 60%	S <sub>37</sub> 312 nm <i>f</i> = 0.18	 47%	 47%
S <sub>24</sub> 340 nm <i>f</i> = 0.27	 22%	 22%	<b>4</b> S <sub>28</sub> 332 nm <i>f</i> = 0.20		
			S <sub>38</sub> 318 nm <i>f</i> = 0.16		

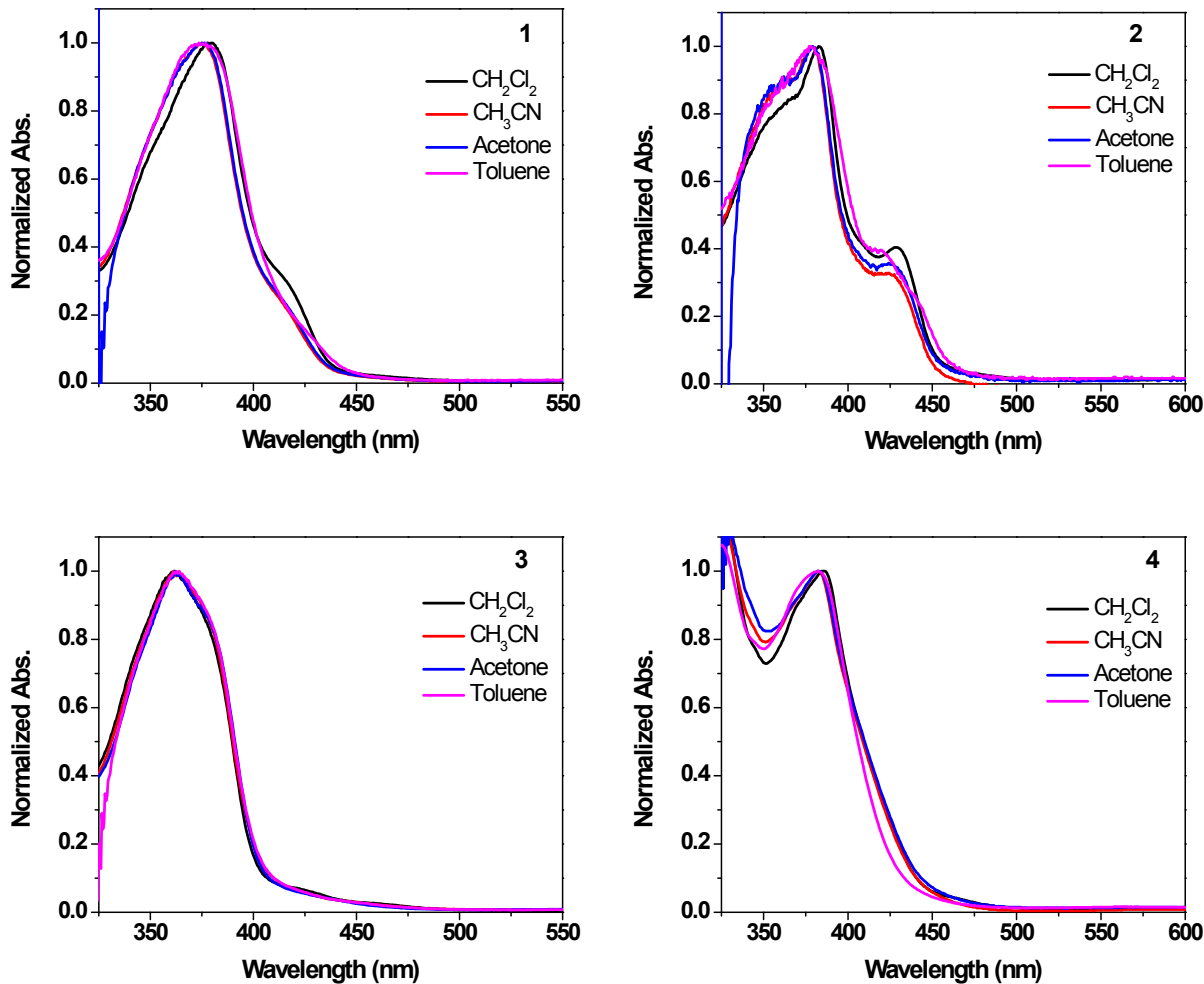


**Figure S4.** Normalized UV-vis absorption spectra of complexes **1 – 4** in different solvents at r.t.

**Table S2.** Emission energies, lifetimes and quantum yields of complexes **1** and **2** in different solvents at R.T.

$\lambda_{\text{em}}$ / nm ( $\tau_{\text{em}}$ / ns; $\Phi_{\text{em}}$ )				
	CH <sub>3</sub> CN	CH <sub>2</sub> Cl <sub>2</sub>	Toluene	Acetone
<b>1</b>	701 (102; 0.041)	704 (192; 0.066)	688 (64; 0.028)	702 (112; 0.048)
<b>2</b>	753 (29; 0.008)	742 (61; 0.024)	- (-; -)	752 (26; 0.010)

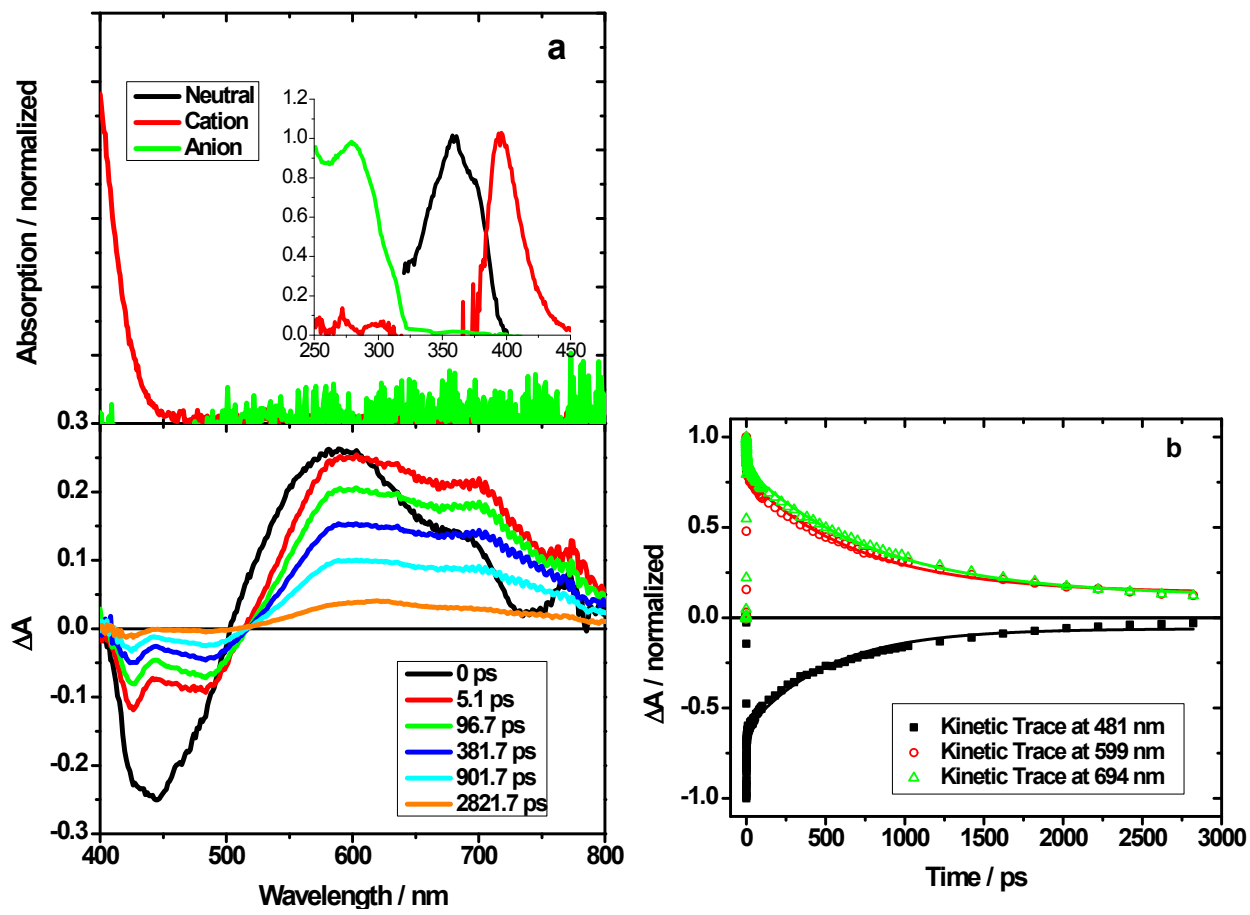


**Figure S5.** (a) Top Panel: Absorption spectra of the neutral (black), cation (red), and anion (green) of ligand **6**. Bottom Panel: Time-resolved fs TA spectra of **6** at various time delays after 390 nm excitation (noted in legend). The inset shows the steady state absorption from 250 to 450 nm. (b) Kinetic traces and their fits for **6**. The parameters of these fits are summarized in Table S3 below.

**Table S3.** Kinetic fit of ligand **6**.

$\lambda$ / nm	$\tau_1$ / ps	$\tau_2$ / ps
481	$2.03 \pm 0.06$	$510.8 \pm 14.4$
599	$5.5 \pm 0.3$	$706.4 \pm 16.5$
694	$4.0 \pm 0.2$	$812.5 \pm 20.1$

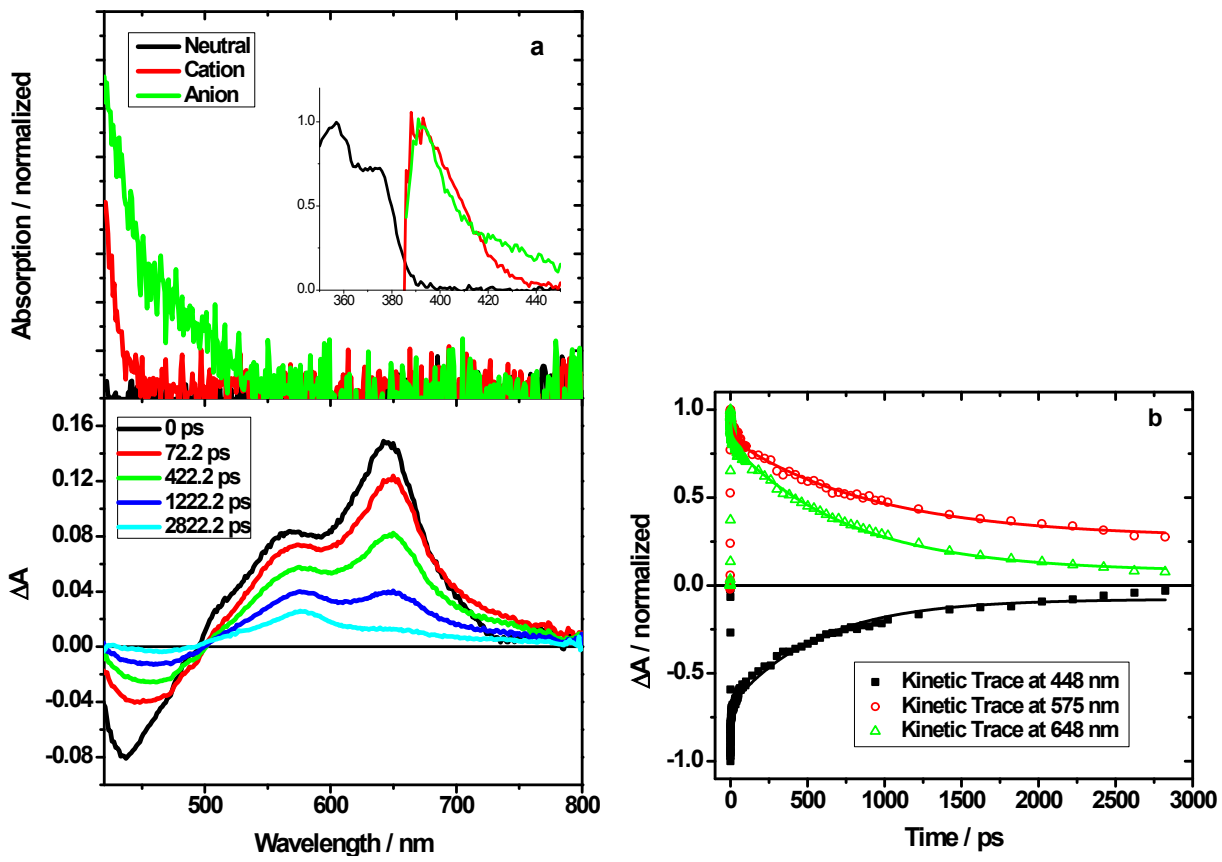


**Figure S6.** (a) Top Panel: Absorption spectra of the neutral (black), cation (red), and anion (green) of ligand 7 in  $\text{CH}_2\text{Cl}_2$ . Bottom Panel: Time-resolved fs TA spectra of 7 at various time delays after 390 nm excitation (noted in legend). The inset shows the steady state absorption from 350 to 450 nm. (b) Kinetic traces and their fits for 7. The parameters of these fits are summarized in Table S4 below.

**Table S4.** Kinetic fit of ligand 7.

$\lambda$ / nm	$\tau_1$ / ps	$\tau_2$ / ps
448	$4.2 \pm 0.3$	$562.0 \pm 20.6$
575	$31.8 \pm 6.8$	$942.9 \pm 63.7$
648	$7.4 \pm 0.4$	$762.0 \pm 17.0$

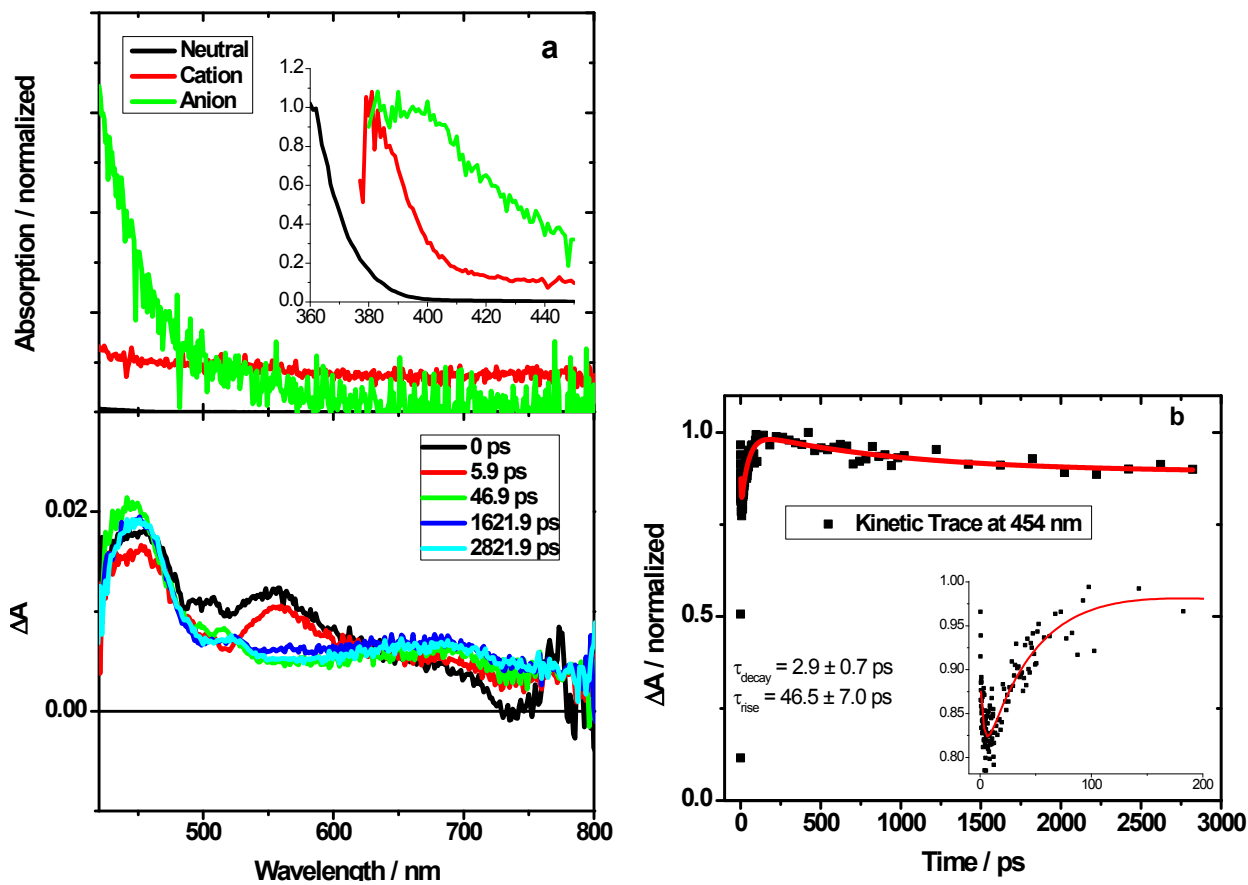


**Figure S7.** (a) Top Panel: Absorption spectra of the neutral **quqo** (black), cation (red), and anion (green). Bottom Panel: Time-resolved fs TA spectra of **quqo** at various time delays after 390 nm excitation (noted in legend). The inset shows the steady state absorption from 300 to 450 nm. (b) Kinetic traces and their fits for **quqo**. Kinetics was measured at 454 nm (black squares). The inset shows an enhanced view of the first 200 ps. In addition to the fast decay with a lifetime of  $\sim 3$  ps followed by a rise with a lifetime of  $\sim 46$  ps, there was a final decay that could not be measured within our time window.

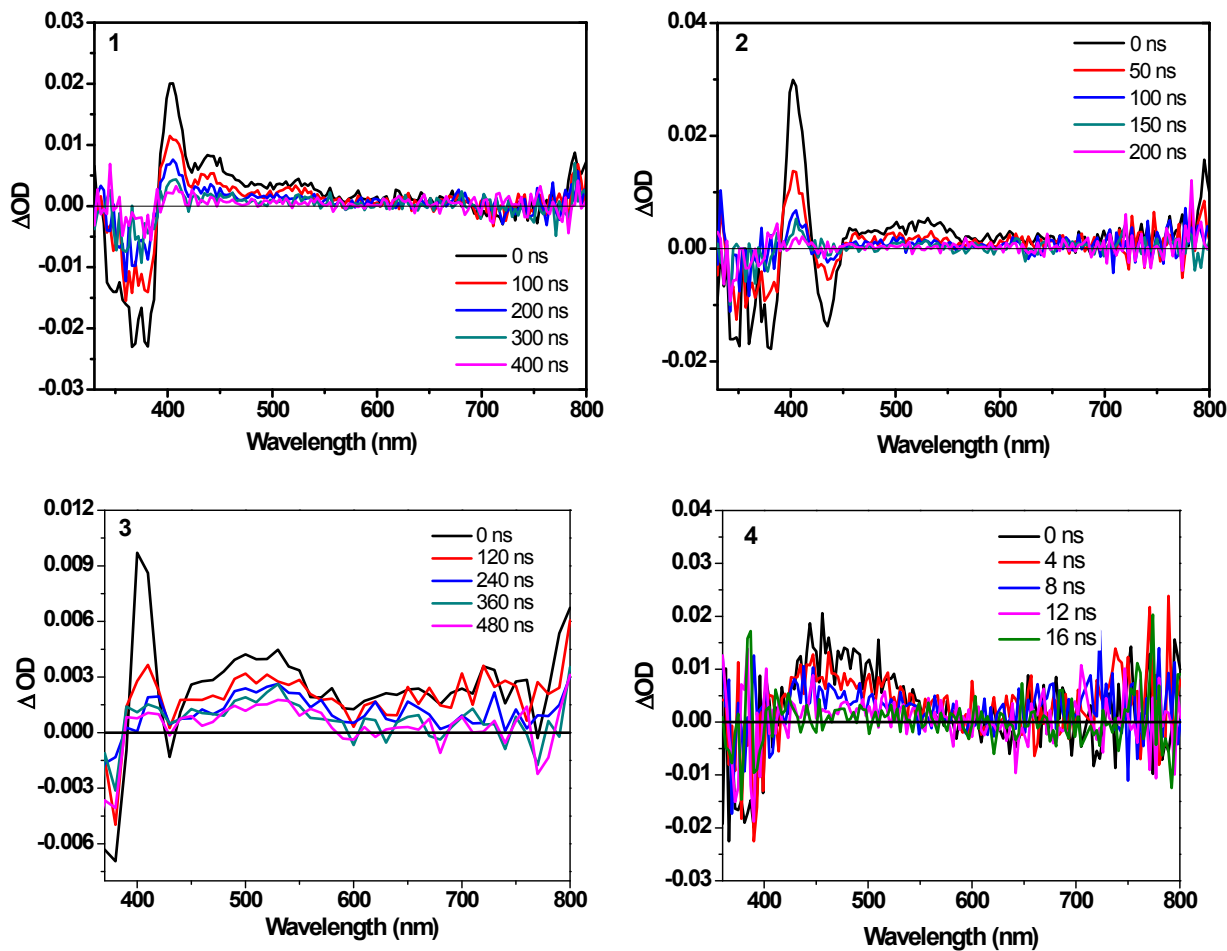


**Figure S8.** Time-resolved ns TA spectra of complexes **1 – 4** in  $\text{CH}_2\text{Cl}_2$ . The excitation wavelength was 355 nm, and the absorbance of the sample solutions was adjusted to 0.4 at 355 nm in a 1-cm cuvette.

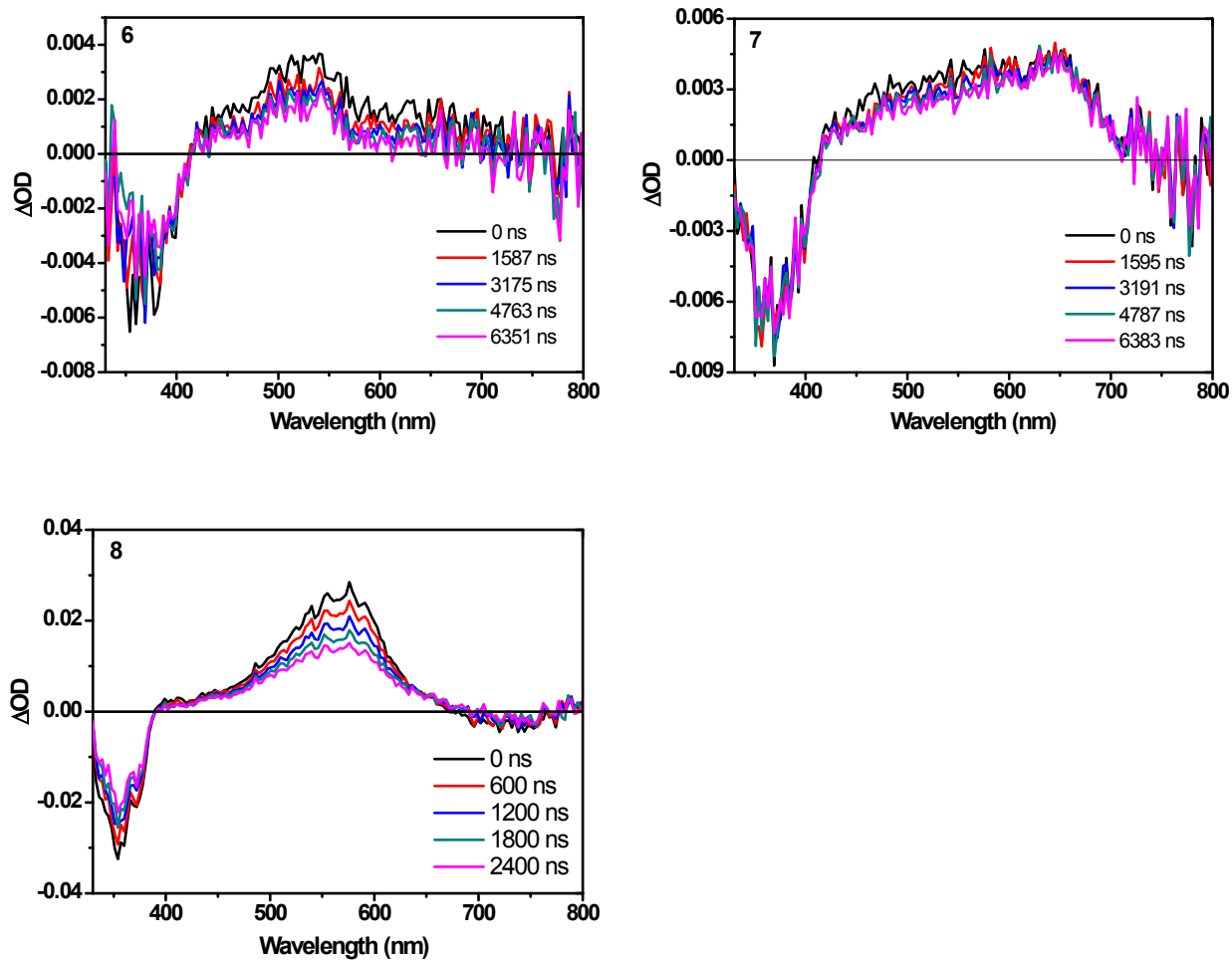


**Figure S9.** Time-resolved ns TA spectra of ligands **6** – **8** in  $\text{CH}_2\text{Cl}_2$ . The excitation wavelength was 355 nm, and the absorbance of the sample solutions was adjusted to 0.4 at 355 nm in a 1-cm cuvette.